

AD-A147 842

ALUMINUM NITRIDE INSULATOR FOR III-V MIS
(METAL-INSULATOR-SEMICONDUCTOR). (U) ROCKWELL
INTERNATIONAL THOUSAND OAKS CA MICROELECTRONICS RESE..

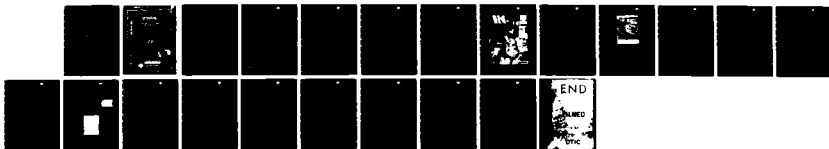
1/1

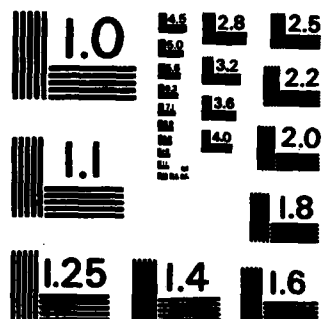
UNCLASSIFIED

K R ELLIOTT ET AL. SEP 84 MRDC41116.1IR

F/G 20/12

NL





MICROCOPY RESOLUTION TEST CHART
NATIONAL BUREAU OF STANDARDS - 1963 - A

**RESEARCH REPORT FOR M-V
AND APPLICATIONS**

**INTERNAL REPORT FOR THE PERIOD
July 1962 through June 1963**

CONTRACT NO. F49620-62-C-0034

Prepared for

**Air Force Office
of Scientific Research
Building 490
Washington, D.C. 20332**

K.R. Elliott, R.W. Grant and M.D. Lind

SEPTEMBER 1964

Approved for public release; distribution unlimited



Rockwell International

**DTIC
ELECTE
NOV 27 1964
S E D**

DTIC FILE COPY

84 11 20 06 7

UNCLASSIFIED

SECURITY CLASSIFICATION OF THIS PAGE

REPORT DOCUMENTATION PAGE

1a. REPORT SECURITY CLASSIFICATION Unclassified		1b. RESTRICTIVE MARKINGS													
2a. SECURITY CLASSIFICATION AUTHORITY		3. DISTRIBUTION/AVAILABILITY OF REPORT Approved for public release; distribution unlimited.													
2b. DECLASSIFICATION/DOWNGRADING SCHEDULE															
4. PERFORMING ORGANIZATION REPORT NUMBER(S) MRDC41116.11R		5. MONITORING ORGANIZATION REPORT NUMBER(S) AFOSR-TR- 84 - 0974													
6a. NAME OF PERFORMING ORGANIZATION Rockwell International Microelectronics Research and Development Center	6b. OFFICE SYMBOL (If applicable)	7a. NAME OF MONITORING ORGANIZATION AFPRO Rockwell International Corporation													
6c. ADDRESS (City, State and ZIP Code) 1049 Camino Dos Rios Thousand Oaks, California 91360		7b. ADDRESS (City, State and ZIP Code) 3370 Miraloma Avenue Anaheim, California 92803													
8a. NAME OF FUNDING/SPONSORING ORGANIZATION Air Force Office of Scientific Research	8b. OFFICE SYMBOL (If applicable) NE	9. PROCUREMENT INSTRUMENT IDENTIFICATION NUMBER Contract No. F49620-82-C-0034													
8c. ADDRESS (City, State and ZIP Code) Bolling AFB Washington, D.C. 20332		10. SOURCE OF FUNDING NOS. <table border="1"><tr><td>PROGRAM ELEMENT NO.</td><td>PROJECT NO.</td><td>TASK NO.</td><td>WORK UNIT NO.</td></tr><tr><td>61102F</td><td>2306</td><td>81</td><td></td></tr></table>		PROGRAM ELEMENT NO.	PROJECT NO.	TASK NO.	WORK UNIT NO.	61102F	2306	81					
PROGRAM ELEMENT NO.	PROJECT NO.	TASK NO.	WORK UNIT NO.												
61102F	2306	81													
11. TITLE (Include Security Classification) A1N INSULATOR FOR III-V MIS APPLICATIONS(U)															
12. PERSONAL AUTHOR(S) Elliott, K.R.; Grant, R.W.; and Lind, M.D.															
13a. TYPE OF REPORT Interim Report	13b. TIME COVERED FROM 07/82 TO 06/83	14. DATE OF REPORT (Yr., Mo., Day) SEPTEMBER 1984	15. PAGE COUNT 21												
16. SUPPLEMENTARY NOTATION P6Sub3															
17. COSATI CODES <table border="1"><tr><td>FIELD</td><td>GROUP</td><td>SUB GR.</td></tr><tr><td></td><td></td><td></td></tr><tr><td></td><td></td><td></td></tr><tr><td></td><td></td><td></td></tr></table>		FIELD	GROUP	SUB GR.										18. SUBJECT TERMS (Continue on reverse if necessary and identify by block number) A1N, MIS, Reactive MBE, A1N Deposition, C-V Analysis.	
FIELD	GROUP	SUB GR.													
19. ABSTRACT (Continue on reverse if necessary and identify by block number) A reactive molecular beam epitaxial (MBE) process has been developed to deposit A1N on GaAs substrates. A1N films on GaAs are being investigated for possible metal-insulator-semiconductor (MIS) applications. Following chemical etching, atomically clean GaAs substrates are prepared by thermal cleaning in ultra-high vacuum. A1N is grown by using Al and NH3 sources. In situ Auger electron analysis shows no detectable oxygen or carbon contamination in the A1N films. Auger and x-ray analysis are used to confirm the A1N stoichiometry. The A1N is crystalline and has the wurtzite type of crystal structure which is hexagonal with space group P63 mc. Far infrared transmission and Raman scattering measurements also identify the films as stoichiometric A1N. Capacitance-voltage measurements for the MIS structures are reported.															
20. DISTRIBUTION/AVAILABILITY OF ABSTRACT UNCLASSIFIED/UNLIMITED <input checked="" type="checkbox"/> SAME AS RPT. <input type="checkbox"/> DTIC USERS <input type="checkbox"/>		21. ABSTRACT SECURITY CLASSIFICATION Unclassified													
22a. NAME OF RESPONSIBLE INDIVIDUAL Kevin J. Malloy, 1Lt, USAF		22b. TELEPHONE NUMBER (Include Area Code) (802) 267-4932	22c. OFFICE SYMBOL NE												



MRDC41116.1IR

TABLE OF CONTENTS

	<u>Page</u>
1.0 INTRODUCTION.....	1
2.0 AlN DEPOSITION APPARATUS.....	2
3.0 AlN PREPARATION.....	4
3.1 Substrate Cleaning.....	4
3.2 AlN Film Formation - Temperature Dependence and Chemistry.....	6
3.3 Al Capping.....	6
3.4 In Contamination.....	7
4.0 AlN PROPERTIES AND CHARACTERIZATION.....	8
4.1 Auger Analysis.....	8
4.2 X-Ray Analysis.....	9
4.3 SEM Analysis.....	9
4.4 XPS Analysis.....	11
4.5 FIR and Raman Analysis.....	12
5.0 ELECTRICAL PROPERTIES OF AlN FILMS.....	14
5.1 Frequency Dispersion.....	14
5.2 Analysis of C-V Data.....	15
6.0 REFERENCES.....	17

Accession For	
NTIS GRA&I	<input checked="" type="checkbox"/>
DTIC TAB	<input type="checkbox"/>
Unannounced	<input type="checkbox"/>
Justification	
By	
Distribution/	
Availability Codes	
Dist	Avail and/or Special
A-1	



AIR FORCE OFFICE OF SCIENTIFIC RESEARCH (AFOSR)
NOTICE OF TRANSMITTAL TO DTIC
This technical report has been reviewed and
approved for public release in accordance with
Distribution is unlimited.
MATTHEW J. KERPER
Chief, Technical Information Division



LIST OF FIGURES

<u>Figure</u>		<u>Page</u>
1	AlN deposition apparatus.....	3
2	SEM micrograph of contaminated surface.....	5
3	Auger electron spectrum of AlN film.....	8
4	Gandolfi x-ray photograph of AlN film.....	10
5	SEM micrograph of clean surface.....	10
6	XPS spectrum of AlN after air exposure.....	11
7	Infrared adsorption spectrum of AlN film.....	12
8	Dispersion of AlN film dielectric constant.....	14
9	C-V data for "best" MIS structure.....	16



MRDC41116.1IR

1.0 INTRODUCTION

This Interim Report discusses progress made during the first year of Contract No. F49620-82-C-0034; the Contract is entitled "AlN Insulator for III-V MIS Applications." If a generally useful MIS technology could be developed for III-V semiconductors, it could have important applications in several digital and analog circuits. The majority of III-V MIS studies have utilized oxides as the insulating gate material. It is frequently observed that these oxides are poor insulators, have substantial trap concentrations and exhibit unacceptably large oxide/III-V interface state densities. These unfavorable characteristics are in general not useful for MIS applications.

The main goal of this program is to investigate the use of AlN as an insulator for III-V MIS applications. AlN has a 6 eV bandgap and has been used successfully as an ion implantation capping material for GaAs. Both Al_{Ga} and N_{As} substitutional sites in GaAs are electrically inactive. AlN is stable in vacuo to high temperature and is also stable in air. In recent years, Fermi level pinning at compound semiconductor interfaces has been attributed by a number of workers to the formation of characteristic defects near or at the interface. The large densities of interface states which are frequently observed in compound semiconductor MIS structures may be associated with the same defects which cause Fermi level pinning. It therefore may be important to utilize an insulator which will minimize defect related interface levels. The use of an isoelectronic wide bandgap III-V material (e.g., AlN) is an attractive possible candidate for this application.

In the following sections we discuss progress related to the development of an AlN/GaAs MIS technology. The AlN deposition apparatus is described in Section 2.0. Investigations of the AlN deposition process are reported in Section 3.0. The characterization of AlN material properties is given in Section 4.0 and measurements of AlN film electrical properties are discussed in Section 5.0.

MRDC41116.11R

2.0 AlN DEPOSITION APPARATUS

A photograph of the AlN deposition apparatus is shown in Fig. 1. The system includes a load lock in order to increase sample throughput and maintain vacuum integrity. By using this load lock, the cycle time of the system is ≈ 2 h per sample. In addition to providing a more efficient means to optimize the deposition process, the load lock improves our ability to decrease background impurity levels.

A Varian MBE 2 in. heated substrate station is utilized to facilitate temperature control of the substrate. Temperature control of the GaAs substrate is an important factor in the AlN deposition process which is discussed in Section 3.2. This heated substrate station considerably improves our ability to reliably control and set the substrate temperature.

An effusion cell has been constructed for the NH_3 source. By monitoring the NH_3 pressure in the cell, it is possible to control the NH_3 flux at the sample surface. A MBE Al source makes it possible to obtain a controlled and stable Al flux. In combination with the load lock mentioned above, the Al source contamination problems are reduced substantially.

In addition, an Auger electron analysis system is attached to the apparatus which makes it possible to monitor the GaAs surface composition prior to deposition and the AlN composition resulting from the deposition.



Rockwell International

MRDC41116.11R

MRDC33-21400

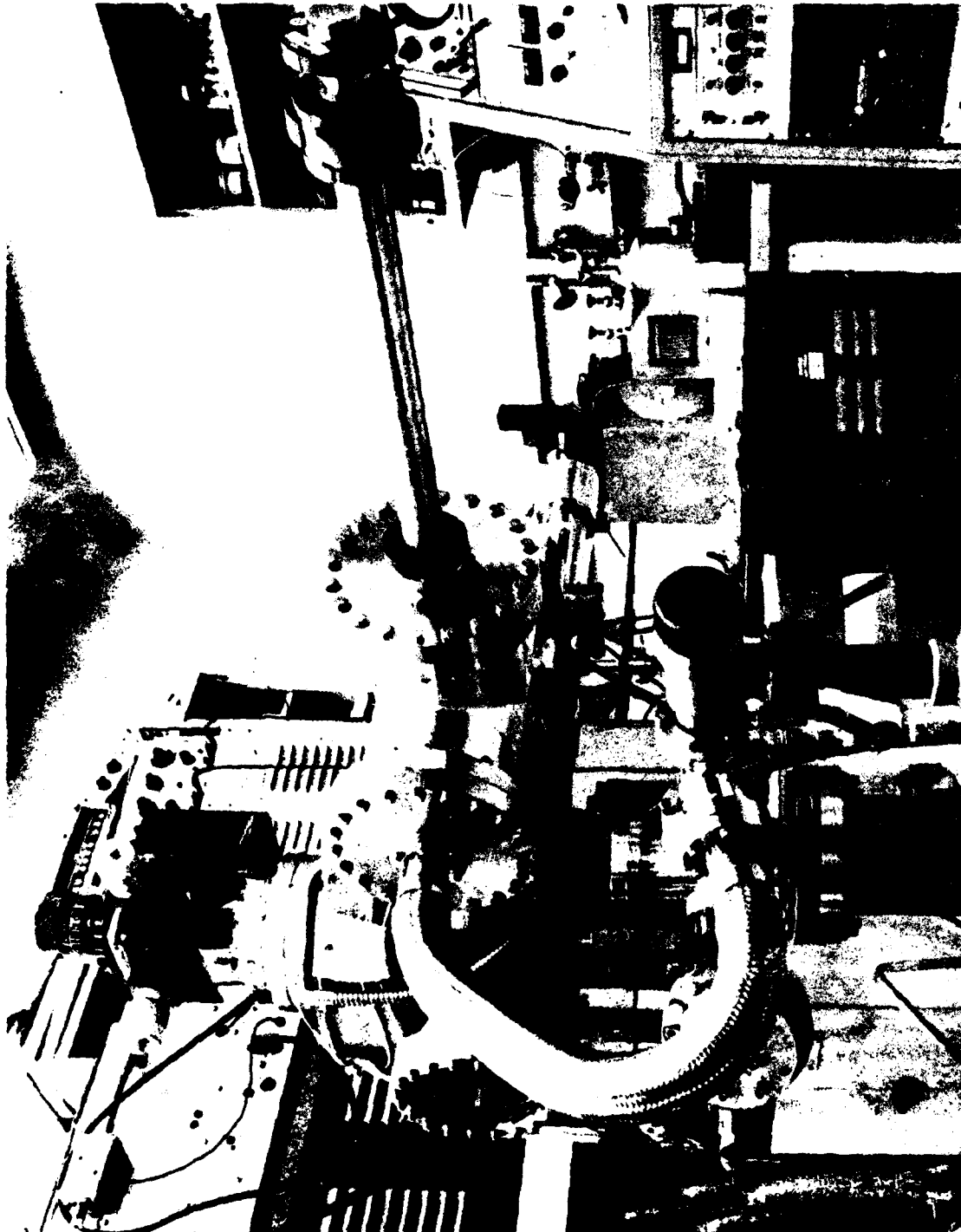


Fig. 1 AlN deposition apparatus.



MRDC41116.11R

3.0 AlN PREPARATION

The apparatus described in the preceding section was developed to investigate the AlN deposition process and to perform in-situ characterization of AlN films by using Auger electron spectroscopy. Substantial progress was made in a number of areas to improve the reproducibility and quality of AlN films produced. In the course of this program, we have identified a number of important conditions which affect film growth. Details of these studies are presented in the following sections.

3.1 Substrate Cleaning

Films have been grown on GaAs (100) oriented substrates which have been cleaned by heating the substrate to temperatures in excess of 600°C. Auger electron analysis of surfaces initially prepared with this method indicated that residual carbon on the substrate was not removed by the heat treatment. In addition, excess carbon from the Auger electron gun was deposited on the substrate during the analysis. Even though such contamination was typically less than a monolayer, the effects of such coverage on the properties of the film were substantial.

SEM micrographs (Fig. 2) show a considerable difference in morphology for regions of a substrate with carbon contamination. This change is visible optically as variations in color of the AlN film across the substrate following deposition, which indicates a change in the optical thickness of the film (film color is due to interference fringes and represents the optical film thickness).

A procedure has been developed for eliminating excess carbon from the surface of the GaAs. As a result, we can obtain GaAs surfaces which are atomically clean as observable by using Auger analysis. This procedure consists of (1) degreasing the GaAs with conventional solvents, (2) etching the GaAs with a $\text{NH}_4\text{OH}:\text{H}_2\text{O}_2:2\text{H}_2\text{O}$ solution and (3) attaching the GaAs substrate to a Mo substrate holder with high purity In. A final step consists of etching the



MRDC33-21489

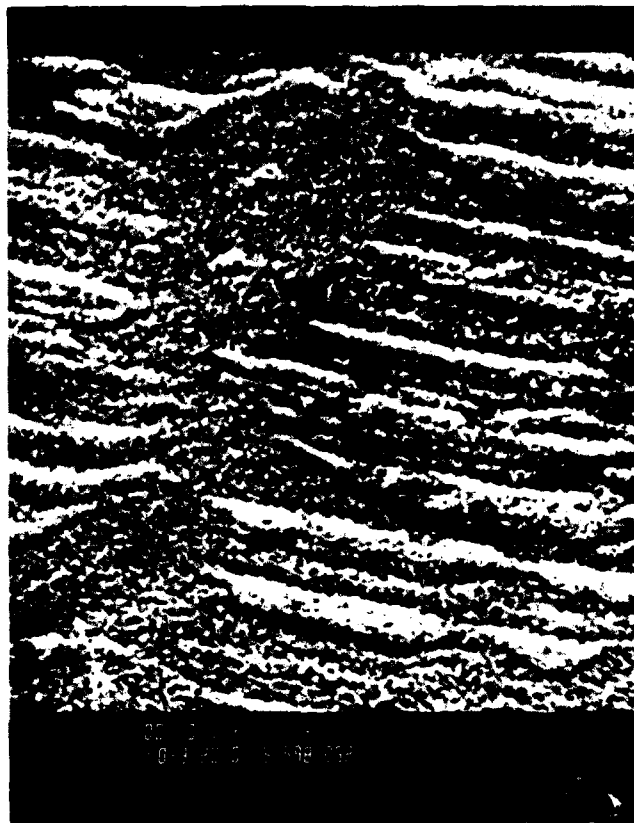


Fig. 2 SEM micrograph of AlN/GaAs film with surface initially contaminated by carbon.

GaAs with a 7:1:1 solution of $\text{H}_2\text{O}:\text{H}_2\text{O}_2:\text{NH}_4\text{OH}$ while spinning the substrate, followed with a rinse of 18 Megohm-cm water and finally spin-drying. The GaAs substrate prepared in this fashion is carbon-free and suitable for heat cleaning.

The thermal stability of the GaAs surface was investigated by heating several samples under UHV at various temperatures. Half of each sample was covered with Si_3N_4 to prevent evaporation from this part of the surface. After



MRDC41116.11R

heating the sample, the Si_3N_4 was removed and the height of each area was compared. These results indicated that GaAs evaporation was negligible at temperatures less than 675°C . At this temperature, roughly 100Å of GaAs evaporated in 30 min, assuming congruent evaporation. No gross deterioration was observed, i.e., the surface remained specular. Therefore, we can conclude that macroscopic degradation of the substrate is negligible at lower temperatures.

3.2 AlN Film Formation - Temperature Dependence and Chemistry

We have made some preliminary studies of AlN formation as a function of substrate temperature. Our results agree with those previously published for growth of AlN on Si. The ammonia flux necessary for stoichiometric film growth increases rapidly below 600°C . For practical conditions, such as growth rates $\sim 100\text{Å}/\text{min}$ and NH_3 partial pressures $< 10^{-3}$ Torr in the system, the temperature for stoichiometric growth must be greater than 550°C . The oxygen desorption temperature of GaAs (which is $\approx 600^\circ\text{C}$) is a convenient temperature for film deposition in that the substrate temperature need not be changed between substrate cleaning and film growth. As discussed in Section 5.2, we have not found a strong correlation to date between the substrate temperature and density of interface states.

3.3 Al Capping

We have developed a technique for protecting the AlN layer from subsequent oxidation. As discussed in Section 4.4, a $\approx 10\text{Å}$ thick layer of oxide forms on the AlN surface upon exposure to air. Traps at the oxide-nitride interface may cause hysteresis in the MIS characteristic. To prevent this kind of trapping, a layer of Al was deposited on the AlN following growth. Such structures have given the "best" C-V characteristics observed to date.



MRDC41116.1IR

3.4 In Contamination

The sample is attached to the substrate holder by wetting both the sample and substrate holder with molten In. During growth, we have discovered that excess In can catastrophically react with AlN to form an Al-In alloy and gaseous nitrogen. The In creeps over the sample surface during this reaction. Although the effect can be eliminated by using less In and a larger sample, the best solution may be to eliminate the In with a different sample holder configuration.

MRDC41116.1IR

4.0 AlN PROPERTIES AND CHARACTERIZATION

AlN films produced in the current program have been characterized by a number of techniques including Auger analysis, x-ray diffraction, SEM, XPS, far infrared transmission and Raman spectroscopy.

4.1 Auger Analysis

The Auger electron spectrometer attached to the growth apparatus has enabled us to characterize the purity of AlN films grown on GaAs in-situ. A typical Auger electron spectrum of an AlN film immediately following growth is shown in Fig. 3. The predominant peaks in the spectrum are associated with Al at 57 eV and N at 381 eV. Oxygen and carbon are not detectable in the spectrum, which indicates that the films have good purity. For the spectrum shown in Fig. 3, we have estimated the composition to be stoichiometric AlN with $[Al]/[N] = 0.94 \pm 0.15$. We can estimate the oxygen content to be less than 0.2% from the same spectrum.

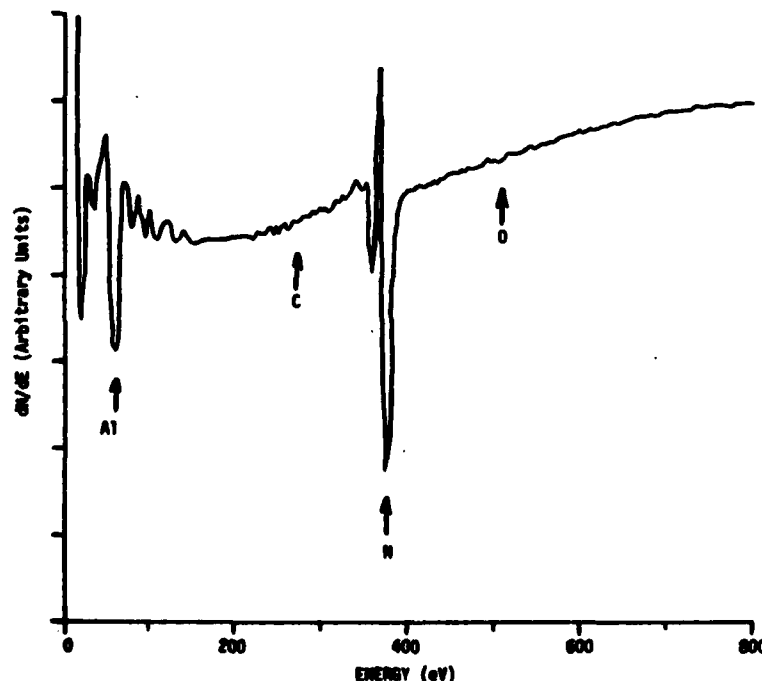


Fig. 3 In-situ Auger electron spectrum of AlN film grown on GaAs. Note the absence of oxygen and carbon in the spectrum.



MRDC41116.1IR

Occasionally, we have observed the presence of Ga and As in the films, particularly for films grown at higher temperatures. We have not detected the presence of other elements in our films.

4.2 X-Ray Analysis

We photographed the $\text{CuK}\alpha$ x-ray diffraction powder pattern of an AlN film with a Gandolfi camera. The sample was approximately a square millimeter in size and had been removed from the substrate. The Gandolfi camera rotates this sample around two axes inclined 45° to one another to generate a series of random orientations as required to photograph the powder pattern. The photograph shown in Fig. 4 is a 72 h exposure. This relatively long exposure time is required because of the relatively small mass of the thin sample. The pattern in Fig. 4 matches the published pattern¹ well. The pattern is that of the wurtzite type of crystal structure, which is hexagonal with space group $P6_3mc$. Lattice parameters measured from the photograph are $a = 3.12 \pm 0.01\text{\AA}$ and $c = 4.98 \pm 0.01\text{\AA}$. These values agree with the published values within the indicated experimental error. The diffraction maxima in the photograph are rather broad; the $\text{K}\alpha_1$ - $\text{K}\alpha_2$ doublet is not resolved. This line broadening is probably the result of strain or the effect of small crystallite size.

4.3 SEM Analysis

As indicated above, the films are composed of crystalline stoichiometric AlN. Scanning electron microscopy (Fig. 5) shows that the films grown with proper substrate preparation (see Section 3.1) have granular morphology with features approximately 1000\AA across. It is possible that we are observing individual crystallites of AlN. Such an interpretation would be consistent with the x-ray results (see Section 4.2).



Rockwell International

MRDC41116.11R

MRDC83-21481

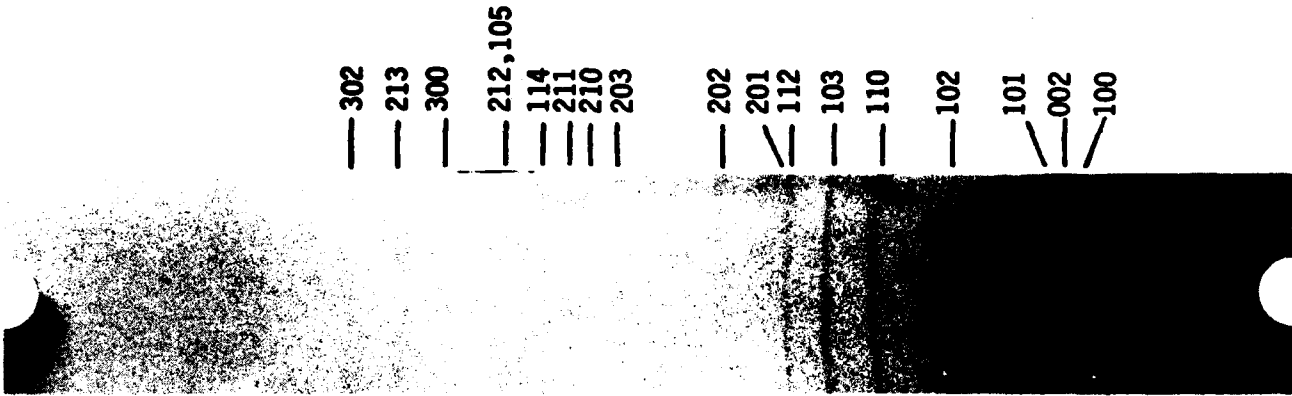


Fig. 4 Gandolfi x-ray photograph of AlN film.

MRDC83-21482

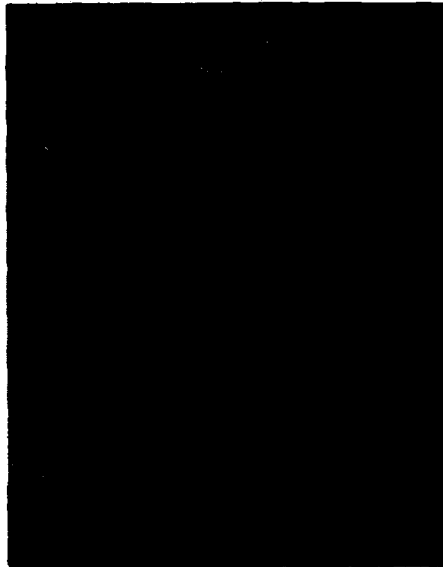


Fig. 5 SEM micrograph of AlN/GaAs film which shows granular morphology.

MRDC41116.11R

4.4 XPS Analysis

X-ray photoemission spectroscopy (XPS) was used to analyze the surface of a thick ($\approx 10^3 \text{ \AA}$) AlN film grown on GaAs (100) in the reactive MBE deposition system (Section 2.0), and subsequently transferred in air into the XPS apparatus. A spectrum is shown in Fig. 6. The substantial O1s signal observed in this spectrum indicates that $\approx 10 \text{ \AA}$ of the surface is oxidized by air exposure. Thus, as mentioned in Section 3.3, it may be important to cap the AlN with a metal before removing it from the MBE system to prevent traps from forming due to the presence of the thin oxidized AlN layer.

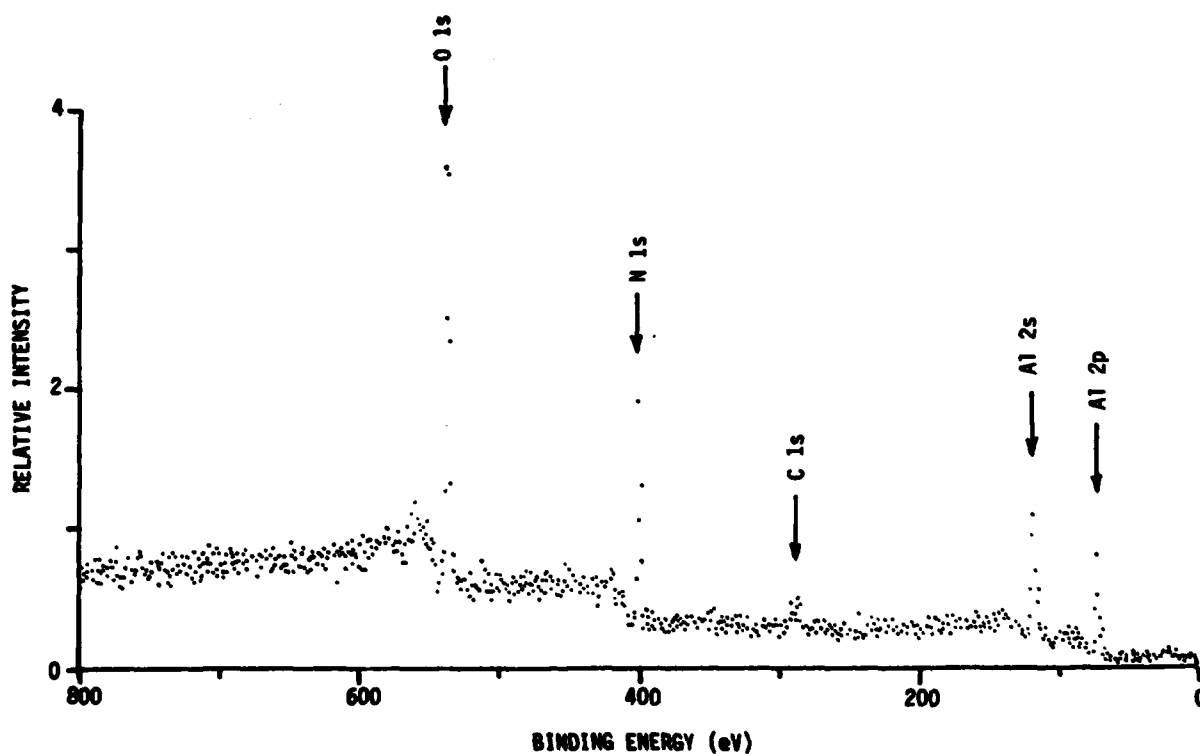


Fig. 6 XPS spectrum of AlN surface after several hours of air exposure.

MRDC41116.1IR

4.5 FIR and Raman Analysis

We have investigated the properties of the AlN films and the GaAs substrate with far infrared transmission (FIR) and Raman scattering spectra. Figure 7 shows a typical transmission spectrum of an AlN layer on a bulk GaAs substrate between 500 cm^{-1} and 1000 cm^{-1} ($20 \text{ }\mu\text{m}$ and $10 \text{ }\mu\text{m}$, respectively).

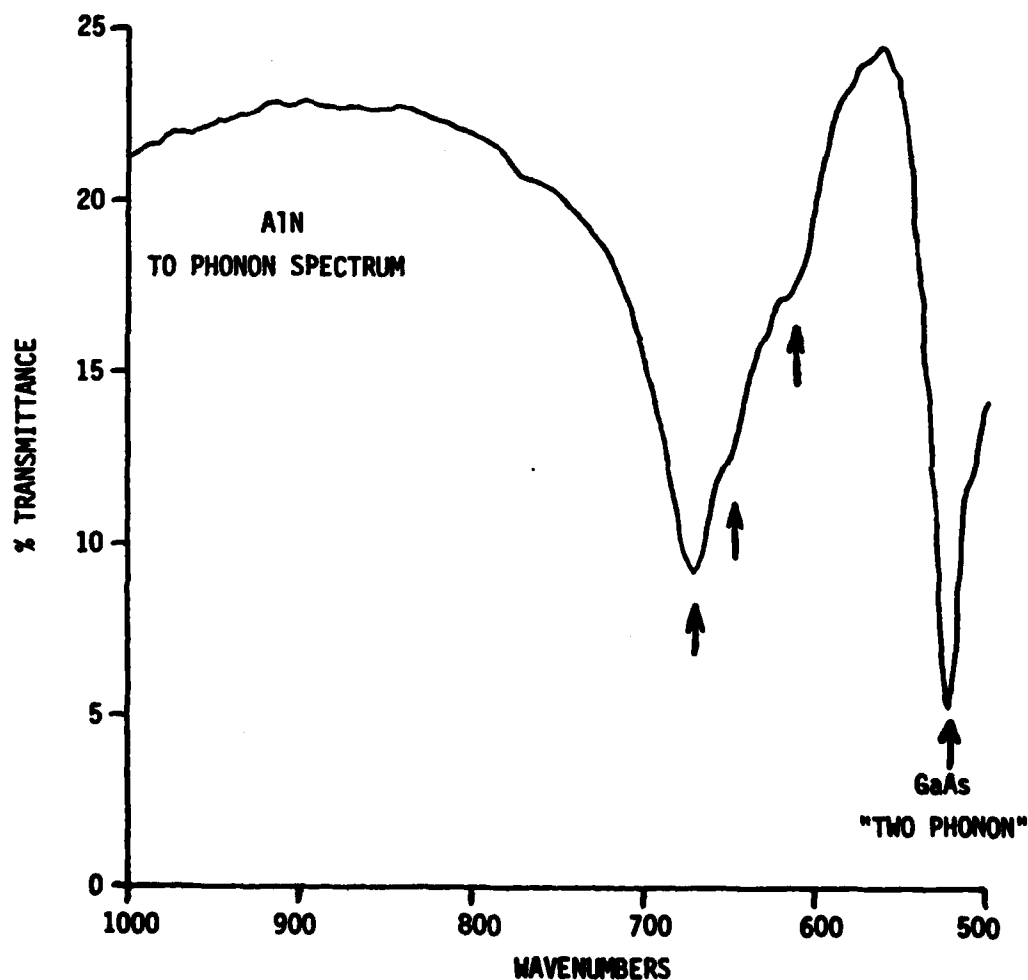


Fig. 7 Infrared absorption spectrum of AlN film grown on GaAs substrate which shows transverse optical modes (marked by arrows) associated with AlN.



MRDC41116.1IR

The GaAs substrate is relatively transparent in this spectral range, except for a two phonon peak at 520 cm^{-1} . The spectrum shows peaks at 610 cm^{-1} , 650 cm^{-1} and 671 cm^{-1} , which corresponds to lattice TO phonons in AlN. These values compare with 610 cm^{-1} , 655 cm^{-1} and 667 cm^{-1} for results obtained on bulk AlN crystals.² These results support the Auger and x-ray analyses which indicate the films consist of stoichiometric crystalline AlN.

We have also looked at Raman spectra of the underlying GaAs substrate. Such spectra have previously been interpreted in terms of strain at the insulator/GaAs interface.³ We observe the GaAs LO phonon mode at 291 cm^{-1} with a width of 7 cm^{-1} . This can be compared with a width of 5 cm^{-1} for a clean GaAs surface. We conclude that strain related broadening of the Raman line is minimal for the AlN deposited on GaAs by reactive deposition.

MRDC41116.11R

5.0 ELECTRICAL PROPERTIES OF AlN FILMS

In this section we analyze electrical and MIS properties of the AlN films grown on GaAs (100).

5.1 Frequency Dispersion

To determine the dielectric properties, variable frequency C-V measurements have been made for AlN films grown on degenerately doped GaAs substrates. The thickness of the films was determined optically and found to be inversely proportional to the capacitance as expected. The results of these measurements are shown in Fig. 8. At low frequencies, the dielectric constant of the insulator increases rapidly. The high frequency dielectric constant corresponds to a value of 8, close to that reported for bulk AlN. A number of explanations can account for this behavior; the most likely is that the dispersion results from conduction associated with trapping centers in the insulator.

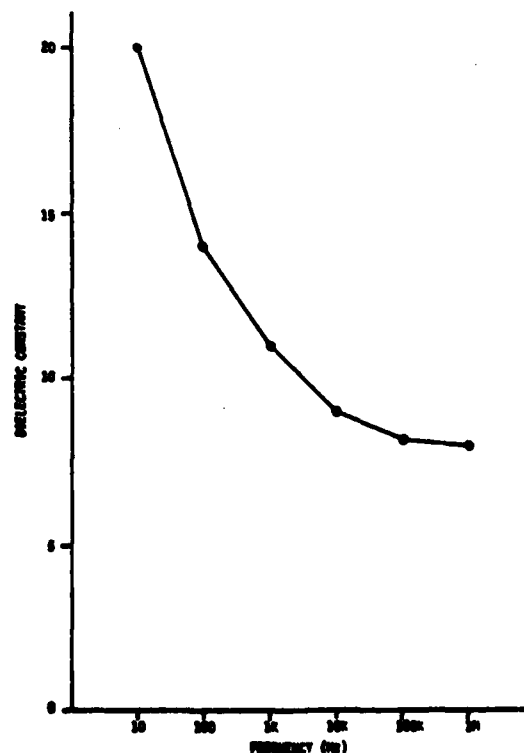


Fig. 8 Dispersion of dielectric constant for AlN film on n^+ GaAs substrate.



MRDC41116.11R

5.2 Analysis of C-V Data

Variable frequency capacitance voltage measurements have been made on a number of samples and analyzed to obtain an effective interface charge density to be used as a figure-of-merit for the C-V results. For the purpose of simplification, this charge density is simply $Q = C_{ins} \Delta V_{FB}$, where Q is the density of interface charge, C_{ins} is the insulator capacitance per unit area, and ΔV_{FB} is the difference from the theoretical flatband voltage. The source of such charge can, in fact, be traps in the insulator or at the semiconductor interface.

For films grown to date, Q has ranged from values as high as 10^{13} cm^{-2} to values as low as $4 \times 10^{11} \text{ cm}^{-2}$ in the "best" samples. The origin of fluctuations in Q has not been determined. We have not been able to correlate Q with either the sample deposition temperature or the Al/NH₃ flux ratio during growth.

A theoretical fit to the "best" C-V curve obtained to date is shown in Fig. 9. The only parameters used to fit the curve are the insulator capacitance and substrate doping. A value of 35 pF was found to agree with the insulator capacitance obtained from the thickness of the layer and the area of the metal dot. The doping level is obtained from fitting the C-V curve in deep depletion. As can be seen from the fit, we appear to obtain inversion between 1.5 and 5 V. Another encouraging aspect of these data is that the hysteresis occurs in a clockwise direction. If the hysteresis was associated with interface states, we would expect hysteresis in the opposite direction, indicating that the primary origin of the hysteresis is not due to interface states, but rather due to charge injection into the insulator or mobile ions. One possible origin of the hysteresis is due to contamination from residual water vapor and other oxygen-containing species in the vacuum system. Another possibility is that a thin oxide layer (formed on the AlN due to air exposure following growth) contributes to the hysteresis.



MRDC41116.1IR

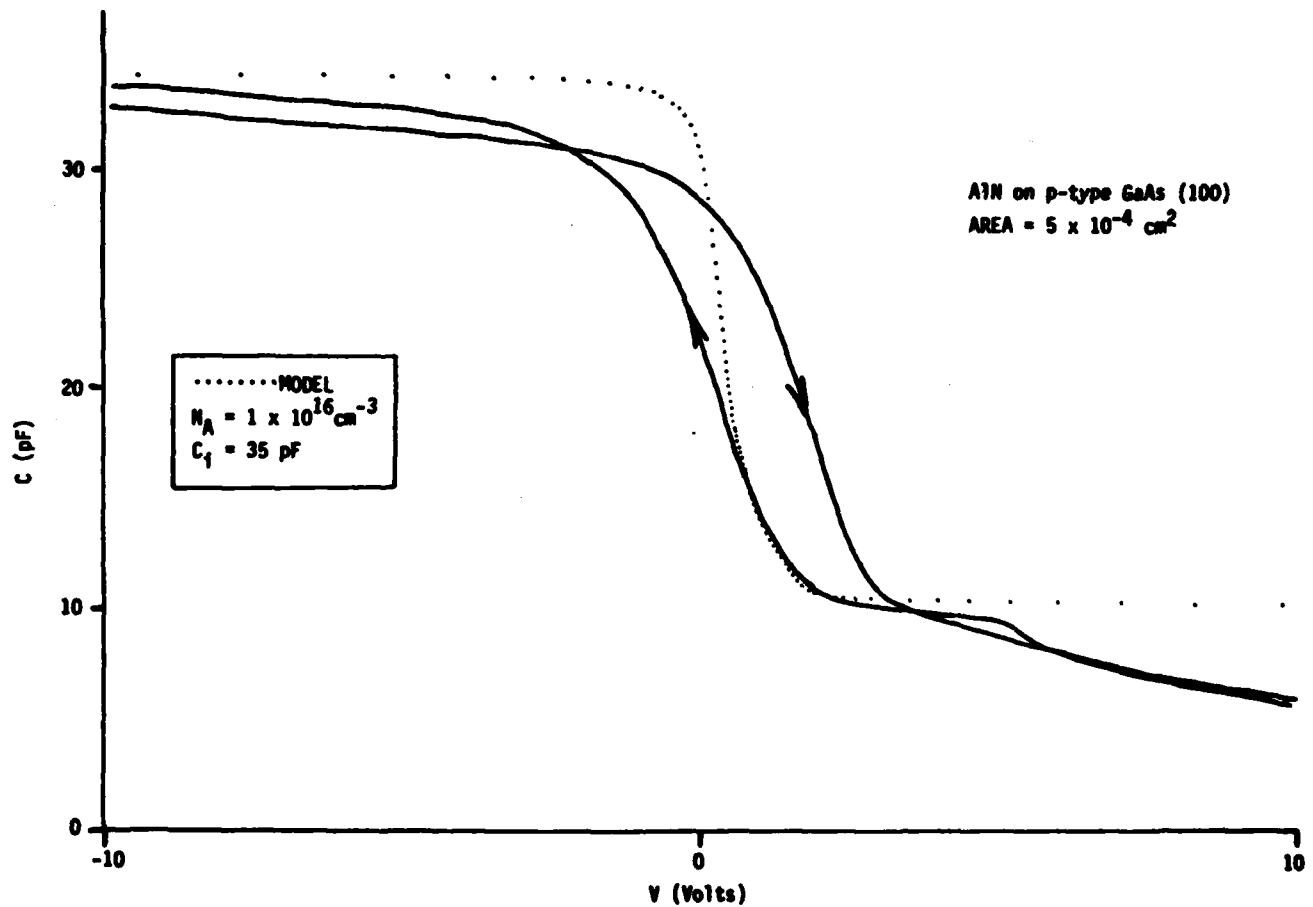


Fig. 9 C-V plot (1 MHz) for "best" MIS structure grown to date. The hysteresis is not consistent with charging of interface states but rather with charge injection or ion migration from the metal gate. A theoretical fit to the data is also shown.



MRDC41116.11R

6.0 REFERENCES

1. Powder Diffraction File, 25-1133, JCPDS International Center for Diffraction Data, Swarthmore, Pennsylvania, 1982.
2. A.T. Collins, E.C. Lightowers and P.J. Dean, Phys. Rev. 158, 833 (1967).
3. H. Nishi, S. Okamura, T. Inada, H. Hashimoto, T. Katoda and T. Nakamura, Inst. Phys. Conf. Ser. N63, 365 (1982).

END

FILMED

12-84

DTIC